

# On the importance of viscous dissipation and heat conduction in binary neutron-star mergers

Mark G. Alford,<sup>1</sup> Luke Bovard,<sup>2</sup> Matthias Hanauske,<sup>2,3</sup> Luciano Rezzolla,<sup>2,3</sup> and Kai Schwenzer<sup>4,5</sup>

<sup>1</sup>Physics Department, Washington University, St. Louis, MO 63130, USA

<sup>2</sup>Institut für Theoretische Physik, Max-von-Laue-Strasse 1, 60438 Frankfurt, Germany

<sup>3</sup>Frankfurt Institute for Advanced Studies, Ruth-Moufang-Strasse 1, 60438 Frankfurt, Germany

<sup>4</sup>Theoretical Astrophysics (IAAT), Eberhard Karls University of Tübingen, Tübingen 72076, Germany

<sup>5</sup>Department of Astronomy and Space Sciences, Istanbul University, Beyazıt, 34119, Istanbul, Turkey

Inferring the properties of dense matter is one of the most exciting prospects from the measurement of gravitational waves from neutron star mergers. However, it will require reliable numerical simulations that incorporate viscous dissipation and energy transport if these can play a significant role within the survival time of the post-merger object. We calculate timescales for typical forms of dissipation and find that thermal transport and shear viscosity will not be important unless neutrino trapping occurs, which requires temperatures above about 10 MeV and gradients over lengthscales of 0.1 km or less. On the other hand, if direct-Urca processes remain suppressed, leaving modified-Urca processes to establish flavor equilibrium, then bulk viscous dissipation could provide significant damping to density oscillations observed right after the merger. When comparing with data from a state-of-the-art merger simulation we find that the bulk viscosity takes values close to its resonant maximum in a typical neutron-star merger, motivating a more careful assessment of the role of bulk viscous dissipation in the gravitational-wave signal from merging neutron stars.

PACS numbers:

*Introduction.* LIGO's first direct detection of gravitational waves from the merger of black holes [1] has improved enormously the prospects for the detection of gravitational waves from neutron-star mergers in the near future. Because neutron stars are extended structures of ultra-dense matter, such observations could contain valuable information about the properties of matter at extreme density and temperature, and the central engine of short gamma-ray bursts (see [2, 3] for reviews). With a few exceptions [4, 5] current numerical simulations of neutron-star mergers neglect the transport properties of the material on the assumption that they will operate on timescales much larger than the dynamical ones of the binary [6]. In this study we revisit this assumption by exploring the impact of shear/bulk viscosity and thermal transport immediately after the merger and by exploiting the results of numerical relativity. These simulations have seen enormous progress in recent years [7–11] and have found that if the total mass of the system is not too large, then the post-merger object is metastable to gravitational collapse over a timescale of tens of milliseconds. The inner region of this object, which is about 10 km across, can reach densities of several times nuclear-matter saturation (number) density  $n_0 \approx 0.16 \text{ fm}^{-3}$  and temperatures of tens of MeV.

The details of the complicated post-merger phase depend on the mass of the system, the equation of state (EOS), and the strength of the magnetic fields that develop after the merger [2, 3]. Quite generically, however, unless it collapses promptly to a black hole [8], the binary-merger product will oscillate in modes that leave a clear imprint on the gravitational-wave signal [12–16]. In such simulations, the large scale motion is damped by gravitational-wave emission over tens of milliseconds. This sets the timescale over which dissipation or transport would have to operate in order to influence the details and duration of the gravitational-wave signal or the emission of neutrinos. Our goal in this *Letter* is to provide simple estimates of the likely effects on the merger

product of the transport properties of the high-density matter. Transport properties vary greatly between different phases, offering the possibility of using data from mergers to probe the phase structure of dense matter, potentially including exotic phases such as quark matter. In particular, we provide estimates of the thermal transport and dissipation timescales over which these processes have a noticeable effect on the system, as a function of relevant properties of the material such as rest-mass density and temperature.

*Thermal equilibration.* To see whether heat diffusion is a significant effect, we first estimate the thermal equilibration time. For this, consider a region of size  $z_{\text{typ}}$  that is hotter than its surroundings by a temperature difference  $\Delta T$ . For a material with specific heat per unit volume  $c_V$  and thermal conductivity  $\kappa$ , this region has an extra thermal energy  $E_{\text{th}} \approx (\pi/6)c_V z_{\text{typ}}^3 \Delta T$  and (assuming a smooth temperature distribution so that the thermal gradient is  $\Delta T/z_{\text{typ}}$ ) heat is conducted out of the region at a rate  $W_{\text{th}} \approx \pi \kappa \Delta T z_{\text{typ}}$ . The thermal equilibration time, namely the time needed to conduct away a significant fraction of the extra thermal energy, is  $\tau_\kappa \equiv E_{\text{th}}/W_{\text{th}} = c_V z_{\text{typ}}^2/(6\kappa)$ . Hence, to evaluate  $\tau_\kappa$  we need estimates of the specific heat and thermal conductivity of beta-equilibrated nuclear matter. The specific heat is dominated by neutrons, which have the largest phase space of low-energy excitations, giving  $c_V \approx 1.0 m_n^* n_n^{1/3} T$ , assuming a Fermi liquid of neutron density  $n_n$  with Landau effective mass  $m_n^*$  [17].

For the thermal conductivity, we recall that in kinetic theory particles of number density  $n_i$ , typical speed  $v_i$ , and mean free path (mfp)  $\lambda_i$ , contribute to the thermal conductivity as  $\kappa \propto \sum_i \kappa_i \propto \sum_i n_i v_i \lambda_i$ , so that  $\kappa$  is effectively dominated by particles with the optimal combination of high density and long mfp. The neutrons, though numerous, are strongly interacting and have a very short mfp. Thermal conductivity is therefore dominated by electrons or neutrinos. At low temperatures, i.e., below a few MeV, the neutrino mfp becomes

longer than the size of the merger region [2, 18], so neutrinos escape and thermal conductivity is dominated by electrons which scatter via exchange of Landau-damped transverse photons. The thermal conductivity is then temperature-independent  $\kappa_e \approx 1.5 n_e^{2/3}/\alpha$  [see Eq. (40) of Ref. [19]], where  $n_e$  is the electron number density and  $\alpha \approx 1/137$  is the fine-structure constant. This yields the thermal equilibration time in the electron dominated regime

$$\tau_\kappa^{(e)} = 4.7 \times 10^8 \text{ s} \left( \frac{0.1}{x_p} \right)^{\frac{2}{3}} \left( \frac{m_n^*}{0.8 m_n} \right) \left( \frac{n_0}{n_n} \right)^{\frac{1}{3}} \left( \frac{z_{\text{typ}}}{1 \text{ km}} \right)^2 \left( \frac{T}{1 \text{ MeV}} \right),$$

where  $x_p \equiv n_e/n_n$  is the proton fraction. Clearly, this timescale is far too large to have an impact on the  $\sim 10$  ms timescale of post-merger processes [2].

At temperatures  $T \gtrsim 10$  MeV, neutrinos become trapped for nucleon density  $n \gtrsim n_0$ , since the neutrino mfp, which at high density depends strongly on in-medium corrections [18, 20], becomes smaller than the star. Electron neutrinos form a degenerate Fermi gas with a Fermi momentum  $p_{F,\nu}$  of about half that of the electrons. Their mfp is longer than that of the electrons, so they dominate the thermal conductivity [21], which is given by  $\kappa_\nu \approx 0.33 n_\nu^{2/3}/(G_F^2 (m_n^*)^2 n_e^{1/3} T)$ , where  $G_F \equiv 1/(293 \text{ MeV})^2$  is the Fermi coupling. This yields the timescale for thermal transport via neutrinos

$$\tau_\kappa^{(\nu)} \approx 0.7 \text{ s} \times \left( \frac{0.1}{x_p} \right)^{\frac{1}{3}} \left( \frac{m_n^*}{0.8 m_n} \right)^3 \left( \frac{\mu_e}{2 \mu_\nu} \right)^2 \left( \frac{z_{\text{typ}}}{1 \text{ km}} \right)^2 \left( \frac{T}{10 \text{ MeV}} \right)^2. \quad (1)$$

In summary, for neutrino-driven thermal transport to be important on a timescale of tens of milliseconds, there would e.g. have to be thermal gradients (e.g., from turbulence) on lengthscales of the order 0.1 km. Moreover, heat transport into cooler regions should manifest itself even more quickly.

*Shear dissipation.* We next estimate the timescale on which shear viscosity plays a role. For this, consider a fluid of rest-mass density  $\rho$  flowing in the  $x$  direction at velocity  $v_x$ , having kinetic energy per unit volume  $E_{\text{kin}} = \frac{1}{2} \rho v_x^2$ . If the fluid has shear viscosity  $\eta$ , then the energy dissipated per unit time and unit volume is  $W_{\text{shear}} \approx \eta (dv_x/dz)^2$ , so that the time needed for shear viscosity to dissipate a significant fraction of the kinetic energy is  $\tau_\eta \equiv E_{\text{kin}}/W_{\text{shear}}$ . To estimate  $\tau_\eta$ , we assume that the flow is fairly uniform, with the velocity varying by a factor of order unity over a distance  $z_{\text{typ}}$  in the  $z$  direction, so  $dv_x/dz \approx v_x/z_{\text{typ}}$  which gives  $\tau_\eta \approx \rho z_{\text{typ}}^2/(2\eta)$ .

In the low-temperature, electron-dominated regime (i.e.,  $T \lesssim 10$  MeV), using the dominant transverse contribution from Ref. [22] [see Eq. (2.4) in Ref. [23]] with the damping scale  $q_t^2 \equiv 4\alpha p_{F,e}^2/\pi$ , we find  $\tau_\eta^{(e)} \approx 0.2 n_e^{14/9}/(\alpha^{5/3} T^{5/3})$ , so

$$\tau_\eta^{(e)} \approx 1.6 \times 10^8 \text{ s} \left( \frac{z_{\text{typ}}}{1 \text{ km}} \right)^2 \left( \frac{T}{1 \text{ MeV}} \right)^{\frac{5}{3}} \left( \frac{n_0}{n_B} \right)^{\frac{5}{9}} \left( \frac{0.1}{x_p} \right)^{\frac{14}{9}}, \quad (2)$$

where  $n_B$  is the baryon number density of nuclear matter. As a result, when electrons dominate, it would take years for the shear viscosity to significantly impact the flow. However, in the high-temperature, neutrino-dominated regime (i.e., for  $T \gtrsim 10$  MeV) neutrinos produce a much larger shear viscosity  $\eta^{(\nu)} \approx 0.46 n_\nu^{4/3}/(G_F^2 (m_n^*)^2 n_e^{1/3} T^2)$  [21], which yields

$$\tau_\eta^{(\nu)} \approx 54 \text{ s} \left( \frac{0.1}{x_p} \right) \left( \frac{m_n^*}{0.8 m_n} \right)^2 \left( \frac{\mu_e}{2 \mu_\nu} \right)^4 \left( \frac{z_{\text{typ}}}{1 \text{ km}} \right)^2 \left( \frac{T}{10 \text{ MeV}} \right)^2, \quad (3)$$

Interestingly, this result depends only indirectly on the density, via the proton fraction  $x_p$  and the ratio of lepton chemical potentials  $\mu_e, \mu_\nu$ . In summary, neutrino shear viscosity could play an important role, i.e.,  $\tau_\eta^{(\nu)}$  could be in the millisecond range, if the neutrino density is anomalously high or if there are flows that experience shear over short distances,  $z_{\text{typ}} \sim 0.01$  km, for example, due to turbulence or high-order non-axisymmetric instabilities [24–27].

*Bulk viscosity.* Next, we study the impact of bulk viscosity, which characterizes the degree to which there is production of heat when a material is compressed or rarefied. We will consider an “averaged” bulk viscosity  $\bar{\zeta}$  in response to a periodic compression-rarefaction cycle. In nuclear matter under compression on millisecond timescales, dissipation arises because the rate of beta equilibration of the proton fraction via Urca processes occurs on the same timescale, allowing the proton fraction to fall out of phase with the applied pressure. As long as the oscillations in the binary-merger product are roughly periodic, we expect that the dissipation induced by pressure variations occurring on a timescale  $t_{\text{dens}}$  can be estimated by using the bulk viscosity evaluated at frequency  $f = 1/t_{\text{dens}}$ . For the interactions of interest here, the bulk viscosity is largest when the internal equilibration rate matches the frequency of the oscillation. Furthermore, because the equilibration rate is sensitive to the temperature, the bulk viscosity shows a resonant maximum as a function of temperature (see, e.g., Fig. 7 in [28]). For oscillations with a timescale  $t_{\text{dens}}$ , the resonant maximum value is [28]

$$\bar{\zeta}_{\text{max}} \equiv Y_\zeta \bar{n} t_{\text{dens}}, \quad Y_\zeta \equiv C^2/(4\pi B \bar{n}), \quad (4)$$

where  $B \equiv -(1/\bar{n}) (\partial \delta\mu/\partial x_p)|_n$  and  $C \equiv \bar{n} (\partial \delta\mu/\partial n)|_{x_p}$  are the nuclear susceptibilities with respect to baryon density and proton fraction, where the chemical potential  $\delta\mu \equiv \mu_n - \mu_p - \mu_e$  characterises the degree to which the system is out of beta equilibrium. This maximum value  $\bar{\zeta}_{\text{max}}$  depends only on properties of the EOS, that is, it is *independent* of the flavor re-equilibration rate. Changing the re-equilibration rate moves the curve in Fig. 7 in [28] “horizontally”, changing the temperature at which the maximum value is attained.

We note that the maximum bulk viscosity is a monotonically increasing function of number density and Fig. 1 shows the prefactor  $Y_\zeta$  for nuclear matter obeying various EOSs, all of which can sustain a  $2 M_\odot$  neutron star [29, 30]. Whereas APR [31] is a cold EOS and is included here for comparison, for all the others we use “hot” EOSs calculated using a model of nuclei and interacting nucleons in statistical equilibrium [32]. In addition to the LS220 [33] (typical radius

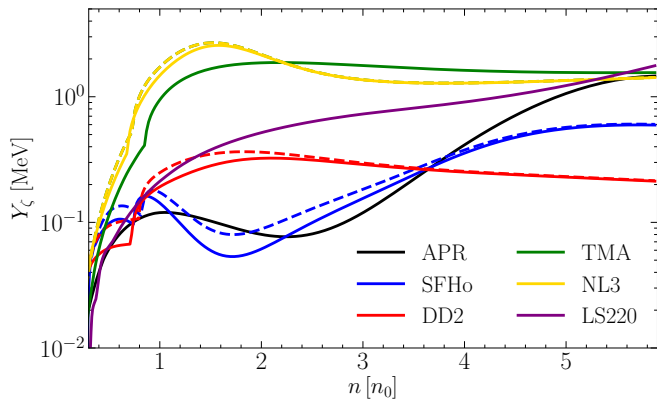


Figure 1: Density dependence of the maximum-bulk-viscosity prefactor  $Y_\zeta$  [see Eq. (4)] for various EOSs. Solid lines are for cold matter ( $T = 0.1$  MeV) while dashed lines are for hot matter ( $T = 10$  MeV). For LS220 we only give a single curve at  $T = 1$  MeV, due to numerical issues in the EOS table.

13 km), used for the simulations below, these EOSs range from the moderately soft SFHo [34], yielding a typical radius of 11 km, through the increasingly stiff DD2 (13 km) [34, 35] and TMA (14 km) [32], to the extremely stiff NL3, with a typical radius of 15 km and a maximum mass of nearly  $3 M_\odot$ . For APR we use a standard quadratic parametrization in terms of the symmetry energy [28] to compute the susceptibilities.

We now show that the temperature  $T_{\zeta_{\max}}$  at which bulk viscosity reaches its resonant maximum for  $\sim 1$  kHz density oscillations (assuming flavor equilibrates via nuclear modified-Urca "nmU" processes) is in the range of temperatures typically found in neutron-star mergers. We recall that for small-amplitude oscillations  $T_{\zeta_{\max}} = (2\pi f / (\tilde{\Gamma} B))^{1/\delta}$  [28], where  $\tilde{\Gamma}$  is the prefactor in the equilibration rate,  $\Gamma = \tilde{\Gamma} T^\delta \delta \mu$ . For modified-Urca processes,  $\delta = 6$ , so  $1/\delta$  is small, making  $T_{\zeta_{\max}}$  insensitive to details of the EOS. As a result, over the relevant frequency range, i.e., from a few tenths to several kHz, we find for "nmU" processes

$$T_{\zeta_{\max}}^{\text{nmU}} \approx 4 - 7 \text{ MeV} \approx 5 - 8 \times 10^{10} \text{ K}, \quad (5)$$

which is well within the range of temperatures expected for dense matter in the post-merger [2, 36, 37].

It should be noted that flavor re-equilibration might instead occur via direct-Urca reactions, which are orders of magnitude faster than modified-Urca processes, giving much lower bulk viscosities at  $T \sim 5$  MeV, since the resonant maximum of bulk viscosity would have moved to lower temperatures (see Fig. 7 in Ref. [28]). In neutrino-transparent matter at  $T = 0$ , direct-Urca processes are allowed when  $\Delta p_F \equiv p_{F,n} - p_{F,p} - p_{F,e} < 0$ . In Fig. 2 we plot this kinematic constraint as a function of density for the same EOSs in Fig. 1. For softer EOSs (e.g., SFHo, DD2) direct-Urca processes are never possible at  $T = 0$ ; however, for APR the direct-Urca channel opens at  $n > 5 n_0$  and for even stiffer EOSs (e.g., NL3, TMA) it already opens below twice saturation density. These considerations suggest that the amount of bulk-viscous damping will be a sensitive indicator of whether

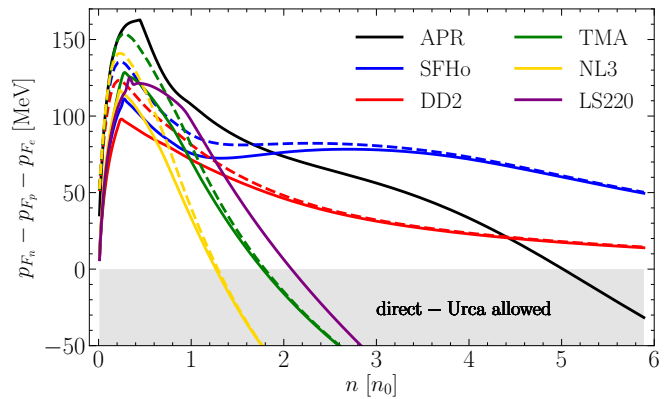


Figure 2: Momentum difference relevant to the direct-Urca channel as a function of density, for the EOSs shown in Fig. 1. For negative values, direct-Urca processes are allowed (grey-shaded area).

the EOS allows direct Urca processes at the densities and temperatures prevalent in neutron star mergers. To draw a more precise connection to the EOS will require calculations of the beta equilibration rate that incorporate the effects of temperature, strong interactions, and the gradual opening of phase space above the direct Urca threshold. The rest of our analysis will focus on showing that if the direct-Urca channel is not open, then bulk viscosity can be expected to have significant effects on the evolution of the post-merger object.

We now estimate the dissipation time for compression oscillations. The energy density for a baryon number-density oscillation of amplitude  $\Delta n$  around average density  $\bar{n}$  is  $\mathcal{E}_{\text{comp}} \approx K \bar{n} (\Delta n / \bar{n})^2 / 18$  [38], where  $K$  is the nuclear compressibility at that density. If the compression varies on a timescale  $t_{\text{dens}}$ , then, in a material with bulk viscosity  $\bar{\zeta}$ , the dissipated power per unit volume is [39]  $(d\mathcal{E}/dt)_{\text{bulk}} \approx 2\pi^2 \bar{\zeta} (\Delta n / \bar{n})^2 / t_{\text{dens}}^2$ . Hence, the time required for bulk viscosity to have a significant impact on the oscillations of the system is

$$\tau_\zeta \equiv \mathcal{E}_{\text{comp}} / (d\mathcal{E}/dt)_{\text{bulk}} \approx K \bar{n} t_{\text{dens}}^2 / (36\pi^2 \bar{\zeta}). \quad (6)$$

Expecting bulk viscosity to reach its maximum value  $\bar{\zeta}_{\max}$  [see Eq. (4)] at typical neutron-star merger temperatures [see Eq. (5)], we can use Eq. (4) in (6) to find that the minimum timescale for bulk viscosity to impact the oscillations is

$$\tau_\zeta^{\min} \approx 3 \text{ ms} \left( \frac{t_{\text{dens}}}{1 \text{ ms}} \right) \left( \frac{K}{250 \text{ MeV}} \right) \left( \frac{0.25 \text{ MeV}}{Y_\zeta} \right). \quad (7)$$

In essence, Eq. (7) reveals that under conditions of maximum bulk viscosity, the damping timescale is a few times larger than the typical timescale  $t_{\text{dens}}$  of density variations.

Since a strong emission of gravitational waves occurs from the high-density region of the star during the first  $\sim 5$  milliseconds after the merger, when characteristic frequencies  $f_1$  and  $f_3$  appear in the gravitational-wave spectrum [14, 16, 41], bulk viscous damping is most likely to have observable consequences if, during that early time, there are density oscillations occurring on a millisecond timescale in parts of the high-

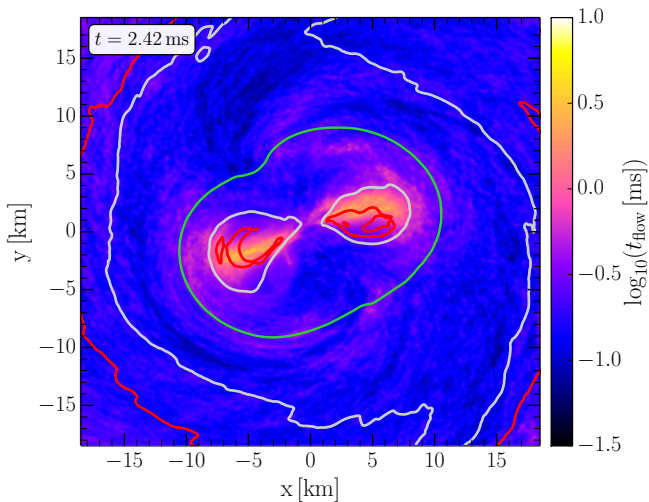


Figure 3: The flow timescale  $t_{\text{flow}}$  obtained from a numerical-relativity simulation of two  $1.35 M_{\odot}$  neutron stars [40]. The red (4 MeV) and gray (7 MeV) contours show the boundaries of the temperature range in which the bulk viscosity roughly takes its maximum value, while the green contour shows the inner region where the rest-mass density exceeds nuclear saturation density.

density region where the bulk viscosity is maximal (i.e., for  $T \sim 4\text{--}7$  MeV).

To test whether such conditions are met, we show in Figs. 3 and 4 results from a state-of-the-art simulation of a merger of two  $M = 2 \times 1.35 M_{\odot}$  stars using the LS220 EOS [33], where  $t = 0$  is the time of merger [41]. Figure 3 uses a colorcode to show the expansion flow timescale  $t_{\text{flow}} \equiv 1/(\langle |\vec{\nabla} \cdot \vec{v}| \rangle) = \rho/D_t \rho$  where  $\langle \rangle$  represents a time average over a 2 ms time window and where  $D_t$  is the Lagrangian time derivative in Newtonian hydrodynamics [42]. This quantity is easily measured and, for a harmonic density oscillation, it is related to Eqs. (6) and (7) by  $t_{\text{dens}} \approx (4\Delta n/\bar{n})t_{\text{flow}}$ . Figure 3 reports  $t_{\text{flow}}$  at 2.4 ms after the merger, where the post-merger object is in its violent and shock-dominated transient phase, (see [41] for a mechanical toy model describing this stage of the post-merger). Inside the green contour, the rest-mass density is above nuclear saturation. The red and grey lines are instead temperature contours at 4 MeV and 7 MeV, respectively. Overall, Fig. 3 shows that there are significant regions where Eq. (7) is a valid estimate of the dissipation time because the density is high and the temperature is in the range that maximizes bulk viscosity [Eq. (5)]. Since in these regions  $t_{\text{flow}} \sim 0.1 - 1$  ms and  $\Delta n/\bar{n} \sim 1$ , we conclude that  $t_{\text{dens}} \approx (4\Delta n/\bar{n})t_{\text{flow}} \sim t_{\text{flow}}$ , is indeed in the millisecond range.

This conclusion is reinforced by Fig. 4, which shows the evolution of various local properties of representative tracer particles in the inner region of the merger product [43]. From the top panel, which reports the evolution of the temperature, we see that the tracers all pass through the temperature range of large bulk viscosity (dark and light-grey shaded areas, showing the regions of maximum and up to an order of magnitude smaller dissipation) during the first few millise-

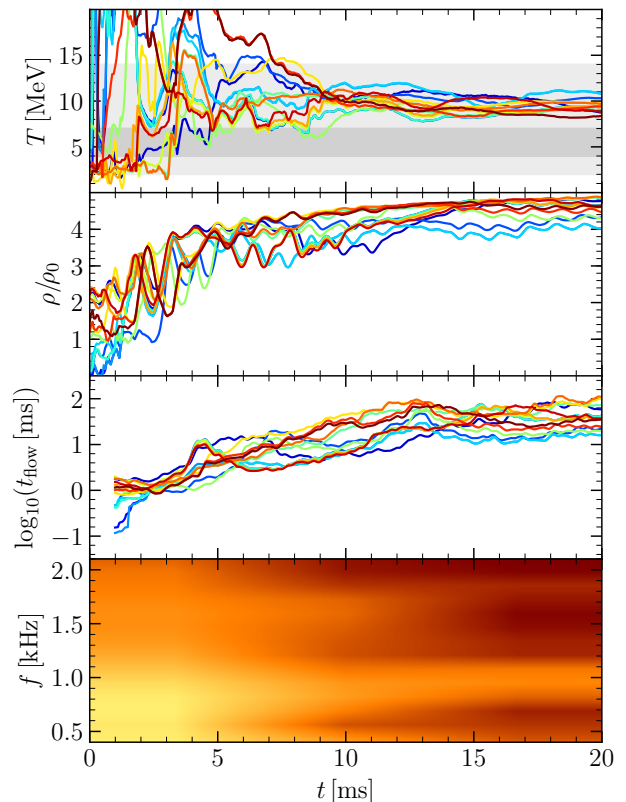


Figure 4: Co-moving time variation of physical properties of post-merger material from selected tracers in the same merger as shown in Fig. 3. Top panel: temperature [the shaded regions are where bulk viscosity is large, see Eq. (5)]. Second panel: rest-mass density. Third panel: flow timescale  $t_{\text{flow}}$ . Bottom panel: spectrogram averaging the rest-mass density evolutions in the second panel.

conds. The second panel reports instead the evolution of the normalized rest-mass density and shows that at early times (i.e.,  $t \lesssim 5$  ms) there are variations of order 100% in the rest-mass density on a timescale of milliseconds, confirming that  $t_{\text{dens}}$  is in that range. The third panel shows the average of  $t_{\text{flow}}$  for the tracers, which is in the 0.1 to 1 ms range, as expected from Figure 3. Finally, the bottom panel of Fig. 4 is a spectrogram averaging the power spectral densities of the normalized rest-mass densities in the second panel and showing how, throughout the first 20 ms, the merger product has oscillation with a significant power at frequencies in the kHz range.

Once again, the results shown in Figs. 3 and Fig. 4, combined with Eq. (7), suggest that if direct Urca processes remain suppressed, then significant bulk viscous dissipation may occur on timescales of order a few milliseconds, which is fast enough to affect the flow of the nuclear material, and hence the emitted gravitational signal. Full numerical-relativity simulations accounting for bulk viscosity are necessary to quantify the amount of such dissipation and its impact on the gravitational-wave signal.

*Conclusions.* Viscous dissipation or thermal transport can play a significant role in neutron-star mergers if the rele-

vant dissipation time is comparable with or shorter than the survival time of the post-merger object, which may range from tens of milliseconds for massive stars up to seconds for lighter ones [2]. Our estimates of dissipation timescales show how they depend on the properties of the post-merger material and on the lengthscale  $z_{\text{typ}}$  over which gradients develop. We find that shear viscosity and thermal conductivity are not likely to play a major role unless neutrino trapping occurs, which requires  $T \gtrsim 10 \text{ MeV}$  and  $z_{\text{typ}} \lesssim 0.01 \text{ km}$ . On the other hand, if direct-Urca processes remain suppressed leaving modified-Urca processes to establish flavor equilibrium, then bulk viscous dissipation could provide significant damping of the high-amplitude density oscillations observed right after merger. Data from a state-of-the-art simulation of a typical merger confirms that the conditions for maximum bulk viscosity are present. We conclude that viscous dissipative processes deserve more careful investigation since they may well affect the spectral properties of the post-merger gravitational-wave signal, especially those peaks that are produced right after the merger and that are dissipated rapidly [12–14, 16, 44]. Since these peaks are routinely employed to infer the properties of the EOS [45, 46], a more realistic treatment of the associated amplitudes is particularly important. In addition, if viscous dissipation is active after the merger, it will also heat the merger product, possibly stabilizing it on longer timescales via the extra thermal pressure [8, 47–49]. If future gravitational-wave observations indicate that the actual dissipation is much smaller than the maximum value leading to Eq. (7), then it would be possible to put limits on how much of the material is in phases where direct Urca is suppressed.

There are various directions in which our research can be further developed. First, the effects of bulk viscosity should

be consistently included in future merger simulations. This has not been attempted before and requires a formulation of the relativistic-hydrodynamic equations that is hyperbolic and stable (see Chap. 6 of [42] for the associated challenges). Second, the bulk viscous effects discussed so far may be amplified by nonlinear suprathreshold enhancement [28, 50–53] or by the even stronger phase-conversion dissipation [54]. Third, because the role played by shear viscosity depends on the typical scale-height of the fluid flow, investigations of the development of turbulent motion in the post-merger phase will be essential (see [55] for a first attempt). Finally, given the vital role they play in determining the strength of thermal transport and shear or bulk viscous dissipation, neutrino trapping and direct-Urca processes motivate additional work to refine constraints on the physical conditions under which these phenomena occur in high-density matter. We plan to consider some of these topics in our future work.

*Acknowledgements.* Support comes from: the U.S. Department of Energy, Office of Science, Office of Nuclear Physics under Award Number #DE-FG02-05ER41375; “NewCompStar”, COST Action MP1304; LOEWE-Program in HIC for FAIR; European Union’s Horizon 2020 Research and Innovation Programme (Grant 671698) (call FETHPC-1-2014, project ExaHyPE). It is a pleasure to thank A. Bauswein, T. Fischer, G. McLaughlin, V. Paschalidis, S. Reddy, A. Sedrakian, S. Shapiro, and P. Shternin for very helpful discussions. MGA and KS acknowledge the hospitality of the Goethe University in Frankfurt, and the of Institute for Nuclear Theory in Seattle during the program INT-16-2b “The Phases of Dense Matter”.

- 
- [1] B. P. Abbott *et al.* (Virgo, LIGO Scientific), *Phys. Rev. Lett.* **116**, 061102 (2016), arXiv:1602.03837 [gr-qc].
- [2] L. Baiotti and L. Rezzolla, *Reports on Progress in Physics* (2016), 10.1088/1361-6633/aa67bb, arXiv:1607.03540 [gr-qc].
- [3] V. Paschalidis, *Classical and Quantum Gravity* **34**, 084002 (2017), arXiv:1611.01519 [astro-ph.HE].
- [4] M. D. Duez, Y. T. Liu, S. L. Shapiro, and B. C. Stephens, *Phys. Rev. D* **69**, 104030 (2004), arXiv:astro-ph/0402502 [astro-ph].
- [5] M. Shibata and K. Kiuchi, arXiv:1705.06142 (2017), arXiv:1705.06142 [astro-ph.HE].
- [6] L. Bildsten and C. Cutler, *Astrophys. J.* **400**, 175 (1992).
- [7] M. Shibata and K. Uryū, *Phys. Rev. D* **61**, 064001 (2000), gr-qc/9911058.
- [8] L. Baiotti, B. Giacomazzo, and L. Rezzolla, *Phys. Rev. D* **78**, 084033 (2008), arXiv:0804.0594 [gr-qc].
- [9] M. Anderson, E. W. Hirschmann, L. Lehner, S. L. Liebling, P. M. Motl, D. Neilsen, C. Palenzuela, and J. E. Tohline, *Phys. Rev. D* **77**, 024006 (2008), arXiv:0708.2720 [gr-qc].
- [10] Y. T. Liu, S. L. Shapiro, Z. B. Etienne, and K. Taniguchi, *Phys. Rev. D* **78**, 024012 (2008), arXiv:0803.4193 [astro-ph].
- [11] S. Bernuzzi, M. Thierfelder, and B. Brügmann, *Phys. Rev. D* **85**, 104030 (2012), arXiv:1109.3611 [gr-qc].
- [12] A. Bauswein and H.-T. Janka, *Phys. Rev. Lett.* **108**, 011101 (2012), arXiv:1106.1616 [astro-ph.SR].
- [13] N. Stergioulas, A. Bauswein, K. Zagkouris, and H.-T. Janka, *Mon. Not. R. Astron. Soc.* **418**, 427 (2011), arXiv:1105.0368 [gr-qc].
- [14] K. Takami, L. Rezzolla, and L. Baiotti, *Phys. Rev. Lett.* **113**, 091104 (2014), arXiv:1403.5672 [gr-qc].
- [15] S. Bernuzzi, T. Dietrich, and A. Nagar, *Phys. Rev. Lett.* **115**, 091101 (2015), arXiv:1504.01764 [gr-qc].
- [16] L. Rezzolla and K. Takami, *Phys. Rev. D* **93**, 124051 (2016), arXiv:1604.00246 [gr-qc].
- [17] K. P. Levenfish and D. G. Yakovlev, *Astronomy Reports* **38**, 247 (1994).
- [18] S. Reddy, M. Prakash, and J. M. Lattimer, *Phys. Rev. D* **58**, 013009 (1998), arXiv:astro-ph/9710115 [astro-ph].
- [19] P. Shternin and D. Yakovlev, *Phys. Rev. D* **75**, 103004 (2007), arXiv:0705.1963 [astro-ph].
- [20] L. F. Roberts and S. Reddy, *Phys. Rev. C* **95**, 045807 (2017), arXiv:1612.02764 [astro-ph.HE].
- [21] B. T. Goodwin and C. J. Pethick, *Astrophys. J.* **253**, 816 (1982).
- [22] P. S. Shternin and D. G. Yakovlev, *Phys. Rev. D* **78**, 063006 (2008), arXiv:0808.2018 [astro-ph].
- [23] C. Manuel and L. Tolos, *Phys. Rev. D* **88**, 043001 (2013), arXiv:1212.2075 [astro-ph.SR].
- [24] K. Kiuchi, P. Cerdá-Durán, K. Kyutoku, Y. Sekiguchi, and

- M. Shibata, *Phys. Rev.* **D92**, 124034 (2015), [arXiv:1509.09205 \[astro-ph.HE\]](#) .
- [25] W. E. East, V. Paschalidis, F. Pretorius, and S. L. Shapiro, *Phys. Rev. D* **93**, 024011 (2016), [arXiv:1511.01093 \[astro-ph.HE\]](#) .
- [26] D. Radice, S. Bernuzzi, and C. D. Ott, *Phys. Rev. D* **94**, 064011 (2016), [arXiv:1603.05726 \[gr-qc\]](#) .
- [27] L. Lehner, S. L. Liebling, C. Palenzuela, and P. M. Motl, *Phys. Rev. D* **94**, 043003 (2016), [arXiv:1605.02369 \[gr-qc\]](#) .
- [28] M. G. Alford, S. Mahmoodifar, and K. Schwenzer, *J. Phys.* **G37**, 125202 (2010), [arXiv:1005.3769 \[nucl-th\]](#) .
- [29] P. Demorest, T. Pennucci, S. Ransom, M. Roberts, and J. Hesses, *Nature* **467**, 1081 (2010), [arXiv:1010.5788 \[astro-ph.HE\]](#) .
- [30] J. Antoniadis, P. C. C. Freire, N. Wex, T. M. Tauris, R. S. Lynch, M. H. van Kerkwijk, M. Kramer, C. Bassa, V. S. Dhillon, T. Driebe, J. W. T. Hessels, V. M. Kaspi, V. I. Kondratiev, N. Langer, T. R. Marsh, M. A. McLaughlin, T. T. Pennucci, S. M. Ransom, I. H. Stairs, J. van Leeuwen, J. P. W. Verbiest, and D. G. Whelan, *Science* **340**, 448 (2013), [arXiv:1304.6875 \[astro-ph.HE\]](#) .
- [31] A. Akmal, V. R. Pandharipande, and D. G. Ravenhall, *Phys. Rev.* **C58**, 1804 (1998), [arXiv:nucl-th/9804027](#) .
- [32] M. Hempel and J. Schaffner-Bielich, *Nucl. Phys.* **A837**, 210 (2010), [arXiv:0911.4073 \[nucl-th\]](#) .
- [33] J. M. Lattimer and F. D. Swesty, *Nucl. Phys.* **A535**, 331 (1991).
- [34] A. W. Steiner, M. Hempel, and T. Fischer, *Astrophys. J.* **774**, 17 (2013), [arXiv:1207.2184 \[astro-ph.SR\]](#) .
- [35] T. Fischer, M. Hempel, I. Sagert, Y. Suwa, and J. Schaffner-Bielich, *Eur. Phys. J.* **A50**, 46 (2014), [arXiv:1307.6190 \[astro-ph.HE\]](#) .
- [36] T. Dietrich and M. Ujevic, ArXiv e-prints (2016), [arXiv:1612.03665 \[gr-qc\]](#) .
- [37] M. Hanauske, K. Takami, L. Bovard, L. Rezzolla, J. A. Font, F. Galeazzi, and H. Stöcker, ArXiv e-prints (2016), [arXiv:1611.07152 \[gr-qc\]](#) .
- [38] T. Klahn *et al.*, *Phys. Rev.* **C74**, 035802 (2006), [arXiv:nucl-th/0602038 \[nucl-th\]](#) .
- [39] R. F. Sawyer, *Phys. Rev.* **D39**, 3804 (1989).
- [40] M. Hanauske, K. Takami, L. Bovard, L. Rezzolla, J. A. Font, F. Galeazzi, and H. Stoecker, (2016), [arXiv:1611.07152 \[gr-qc\]](#) .
- [41] K. Takami, L. Rezzolla, and L. Baiotti, *Phys. Rev. D* **91**, 064001 (2015), [arXiv:1412.3240 \[gr-qc\]](#) .
- [42] L. Rezzolla and O. Zanotti, *Relativistic Hydrodynamics* (Oxford University Press, Oxford, UK, 2013).
- [43] L. Bovard and L. Rezzolla, ArXiv e-prints (2017), [arXiv:1705.07882 \[gr-qc\]](#) .
- [44] F. Maione, R. De Pietri, A. Feo, and F. Löffler, [arXiv:1707.03368 \(2017\)](#), [arXiv:1707.03368 \[gr-qc\]](#) .
- [45] J. A. Clark, A. Bauswein, N. Stergioulas, and D. Shoemaker, *Class. Quantum Grav.* **33**, 085003 (2016), [arXiv:1509.08522 \[astro-ph.HE\]](#) .
- [46] S. Bose, K. Chakravarti, L. Rezzolla, B. S. Sathyaprakash, and K. Takami, [arXiv:1705.10850 \(2017\)](#), [arXiv:1705.10850 \[gr-qc\]](#) .
- [47] Y. Sekiguchi, K. Kiuchi, K. Kyutoku, and M. Shibata, *Phys. Rev. Lett.* **107**, 051102 (2011), [arXiv:1105.2125 \[gr-qc\]](#) .
- [48] V. Paschalidis, Z. B. Etienne, and S. L. Shapiro, *Phys. Rev.* **D86**, 064032 (2012), [arXiv:1208.5487 \[astro-ph.HE\]](#) .
- [49] J. D. Kaplan, C. D. Ott, E. P. O'Connor, K. Kiuchi, L. Roberts, and M. Duez, *Astrophys. J.* **790**, 19 (2014), [arXiv:1306.4034 \[astro-ph.HE\]](#) .
- [50] A. Reisenegger and A. A. Bonacic, (2003), [arXiv:astro-ph/0303454](#) .
- [51] A. A. Bonacic, Master thesis, Universidad Catolica de Chile (2003).
- [52] M. G. Alford, S. Reddy, and K. Schwenzer, *Phys. Rev. Lett.* **108**, 111102 (2012), [arXiv:1110.6213 \[nucl-th\]](#) .
- [53] M. G. Alford and K. Pangeni, *Phys. Rev.* **C95**, 015802 (2017), [arXiv:1610.08617 \[nucl-th\]](#) .
- [54] M. G. Alford, S. Han, and K. Schwenzer, *Phys. Rev.* **C91**, 055804 (2015), [arXiv:1404.5279 \[astro-ph.SR\]](#) .
- [55] D. Radice, *Astrophys. J. Lett.* **838**, L2 (2017), [arXiv:1703.02046 \[astro-ph.HE\]](#) .